Available online at www.sciencedirect.com
SCIENCE DIRECT®
Thin Solid Films 433 (2003) 27–33
thin solid films
www.elsevier.com/locate/tsf

a-C thin film deposition by laser ablation

O. Olea-Cardoso[a], E. Camps[b,*], L. Escobar-Alarcón[b], S. Muhl[c], S.E. Rodil[c], M.A. Camacho-López[d], E. Haro-Poniatowski[d]

[a]*U.A.E.M, Edo. de Mexico, Mexico*
[b]*Departamento de Física, Instituto Nacional de Investigaciones Nucleares, Apartado postal 18-1027, Mexico DF 11801, Mexico*
[c]*Instituto de Investigaciones en Materiales, U.N.A.M., Mexico DF, Mexico*
[d]*Departamento de Física, U.A.M.-I, Mexico DF, Mexico*

Abstract

The plasma formed during the laser ablation of a carbon target has been studied by optical emission spectroscopy and Langmuir electrostatic probes in order to investigate the kinetic energy of the ions, and the plasma density as a function of the target-to-substrate distance and the laser intensity. The experiments were carried out using a Nd:YAG laser with emission at the fundamental line, with a maximum energy output of 150 mJ. In our experimental conditions the plasma emission is principally due to C^+ (283.66, 290.6, 299.2 and 426.65 nm) and C^{2+} (406.89 and 418.66 nm). The ion energies detected varied in a wide range, from ~100 up to 500 eV. The highest plasma densities (9×10^{13} cm^{-3}) that could be detected with the probe were measured at 6 cm from the target, and the lowest (5×10^{11} cm^{-3}) were measured at 15 cm. The characterized plasma regimes were used for the deposition of a-C films under different ion energies and plasma densities, so that different percentages of sp^3 bonding might be formed in the deposits. The films were analysed using Raman spectroscopy, EELS and EDS.

Keywords: Laser ablation; Diamond-like carbon; Optical emission spectroscopy; Langmuir probe

1. Introduction

Diamond-like carbon (DLC) films have attracted substantial attention recently [1,2]. These types of films can be produced by techniques such as chemical vapour deposition (CVD) and pulsed laser deposition (PLD). The PLD technique is known to produce high sp^3/sp^2 bond ratios, with low or no hydrogen content, and that the film characteristics depend on the growth conditions [3]. The commercial use of DLC is at present mainly limited to mechanical applications, which take advantage of the high mechanical hardness, low friction, optical transparency and chemical inertness of the material, due to the presence of the C–C sp^3 bonds. DLC films are also used as protective coatings for magnetic disk drives and anti-reflective protective coatings for IR windows [4]. A potentially promising application of DLC films is in field emission displays [5], where they might be used as the emitter in low-cost flat panel displays.

Diamond-like carbon can only be produced under specific deposition conditions. The theory of the growth models are based on the ideas originally proposed by Lifshitz [6]. Carbon ions with sufficient energy are supposed to be accumulated by subsurface implantation with an accompanying thermal spike. Another microscopic model has been proposed by Robertson [7], in which again subplantation is considered the underlying mechanism. In this model, it was suggested that densification caused by the implantation promoted atomic hybridisations to adjust the local density, favouring the formation of sp^2C in low-density regions and sp^3C formation in the high-density regions. It is considered that subplantation of atoms can either occur by direct implantation of the incoming ions or by knock-on implantation of the surface atoms. The accumulation of atoms in 'interstitial' positions causes an increase in the local density and thus, the local bonding transformations to sp^3 hybridisation to compensate. In order, for the ion to penetrate the film, or cause knock-on implantation, it must have energy above a certain threshold level. It was also suggested, however, that ions of much higher

*Corresponding author. Tel.: +52-5-329-7200x2251; fax: +52-5329-7332.
E-mail address: ecc@nuclear.inin.mx (E. Camps).

0040-6090/03/$ - see front matter © 2003 Elsevier Science B.V. All rights reserved.
PII: S0040-6090(03)00319-5

energies would not promote sp^3 hybridisation because they would cause damage or excessive local heating, which could activate a relaxation in the excess density. Thus, there exists optimum ion energy for maximum sp^3 content, just above the penetration threshold.

The above discussion, indicates that in order to deposit DLC films, a detailed knowledge of the characteristics of the particles used to form the films are necessary. When plasmas are used, this means that a prior diagnostic study of the plasma parameters should be performed and this is one of the main aims of the present article. This work employed Optical Emission Spectroscopy (OES) to study the main excited species present in the plasma during laser ablation of a carbon target. A planar Langmuir probe was used to quantify the mean energy and density of ions, in the position where the substrate was located. The third part of this work is related to the characterization of amorphous carbon films deposited using the diagnosed plasma regimes.

2. Experimental setup

The deposition of the films and the analysis of the plasma, was carried out in a device designed and constructed in our laboratory, and is described in detail elsewhere [8]. Briefly, laser ablation was performed using a Q-switched Nd:YAG laser with emission at the fundamental line ($\lambda = 1064$ nm) with a 28 ns pulse duration. The energy density delivered to the target could be varied from 2 to 6 J/cm^2. The laser beam was focused on the rotating high purity graphite target at an incidence angle of 45°. The 150-mm-diameter vacuum chamber was evacuated to a base pressure of 9.3×10^{-4} Pa. In order to perform experiments at higher pressures, the vacuum chamber was filled with helium up to the necessary pressure.

Optical emission spectroscopy was carried out using a gated intensified CCD, which allowed performing time resolved measurements for the different distances from the target, up to approximately 4 cm, where the plasma

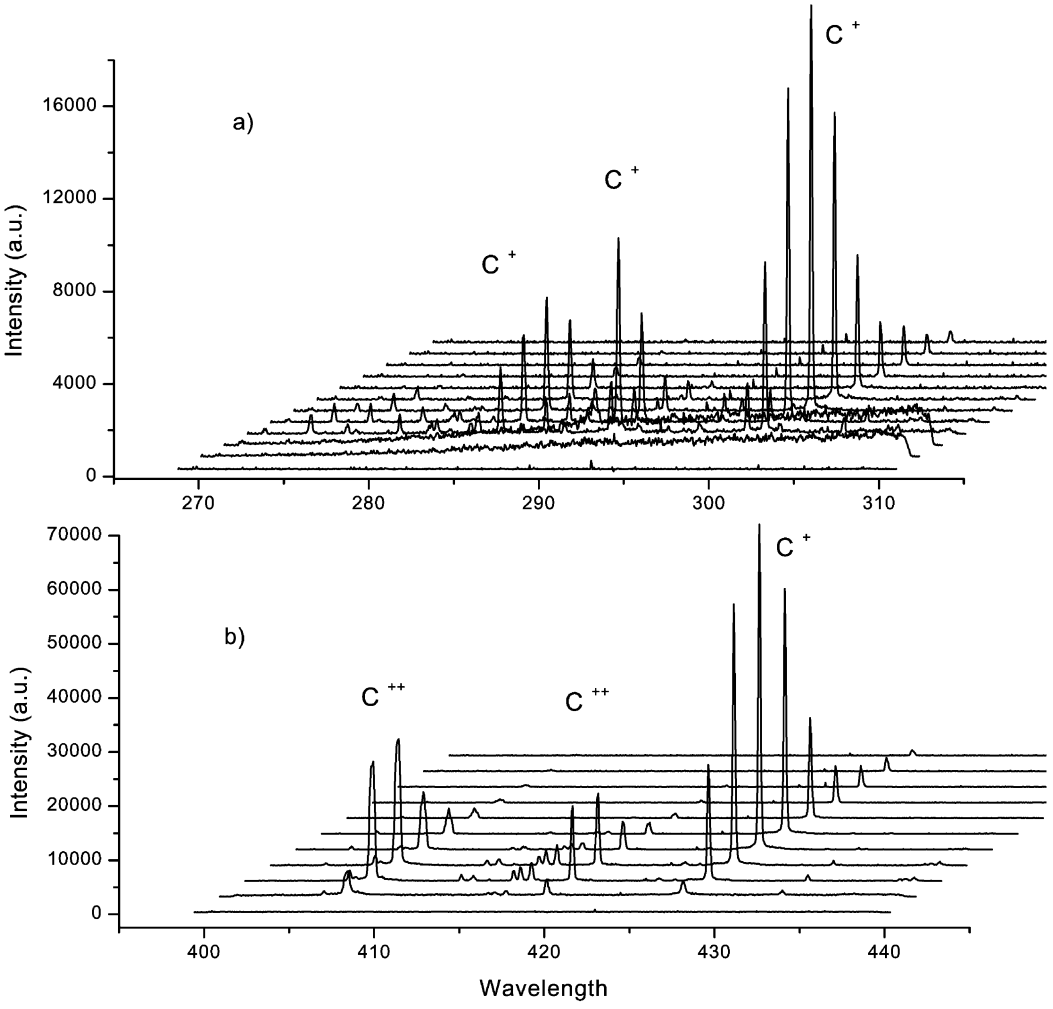

Fig. 1. Time resolved optical emission spectra, for the two spectral regions where plasma emission was detected. In both cases the experimental conditions were: time step between spectra 50 ns, laser fluence 6 J/cm^2, distance from the target 0.5 cm and working pressure 1×10^{-3} Pa.

emission becomes undetectable. The light from the plasma was collected by a system of lenses, focused into a UV–Vis optical fibre bundle and transported to a 0.5 m spectrograph. A 40 μm slit and a 1200 l/mm grating were used throughout. This arrangement allowed a 40 nm spectral window with a 2 Å resolution.

A Langmuir planar probe that could be displaced along the propagation axis (x axis in the following, $x=0$ is the target position) of the plasma plume was used to study, the time of flight of plasma ions and for the determination of the plasma density. Data were recorded from 6 to 15 cm from the target surface. The probe consisted of a 3-mm diameter disk, and was biased with a fixed voltage at −30 V, where saturation of the ion current was evident. The signal from the probe was monitored through a load resistor of 40 Ω and recorded on a fast digital oscilloscope, HP54522A.

The amorphous carbon thin films were deposited on silicon and glass substrates, cleaned in ultrasonic bath of methanol. In order to study the influence of plasma parameters on the characteristics of the deposited material, the films were deposited at different distances from the substrate between 6 and 15 cm, and three values of laser fluence, a low value of 2 J/cm^2, a medium value of 4 J/cm^2 and a high one of 6 J/cm^2. The surface morphology of the samples was examined using a SEM equipped with an EDS probe, which was used to ensure the absence of contamination. Raman spectroscopy measurements were performed at room temperature in air with a Spex 1403 double monochromator using the 514.5 line of an argon laser at a power level of 100 mW in the backscattering configuration. EELS was carried out using a Gatan Image Filtering attached to a JEOL 2010 TEM. The EELS spectra were acquired with 200 kV energy, 0.3 dispersion, in the spectroscopic mode with a 2 mm aperture.

3. Results and discussion

3.1. Plasma diagnostics

Fig. 1a and b shows typical spectra with the spectrograph centered at 290 nm and 420 nm, respectively. These figures show the temporal evolution of the emission at $x=0.5$ cm with a delay time step of 50 ns (i.e. time between strips) and at a pressure of 1×10^{-3} Pa. The emitting species are always the same, no matter what pressure or laser flux is used and they are; C^+ (283.66, 290.6, 299.2 and 426.65 nm) and C^{2+} (406.89 and 418.66), with the C^+ being the most intense which

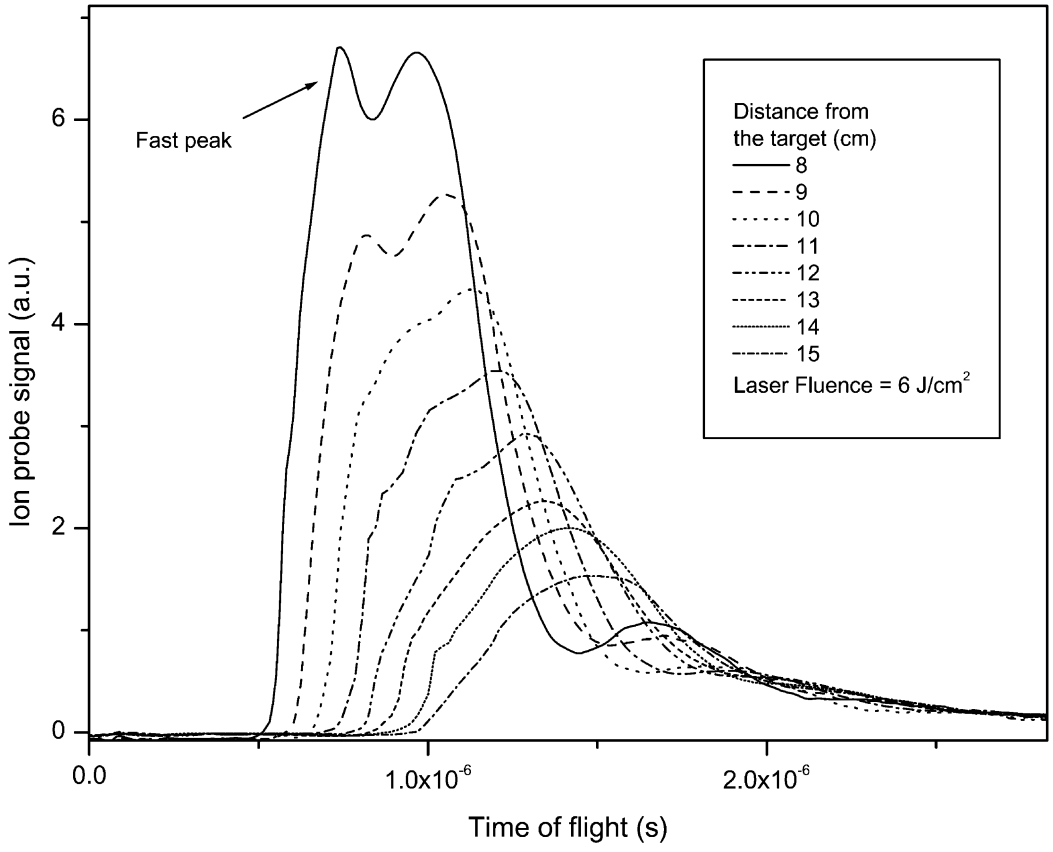

Fig. 2. Time of flight curves of the ion current detected with the Langmuir probe.

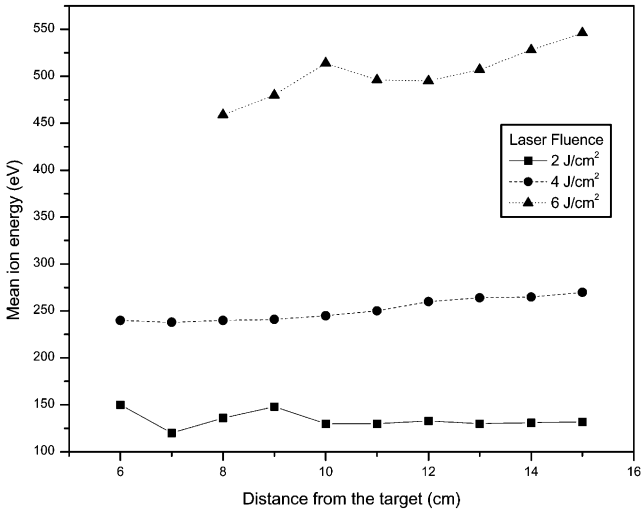

Fig. 3. Mean ion kinetic energy as a function of the distance from the target for different values of laser fluence.

lived for the longest times. Plotting the emission intensity vs. delay time, one can obtain the time of flight (TOF) spectra for each of the emission peaks and the mean kinetic energy of the species was calculated from those curves [9]. For the highest laser fluence used, the mean kinetic energy calculations were performed and they showed an overall behaviour that can be resumed as follows: the mean kinetic ion energy achieves its maximum value of 400 eV at approximately $x=2$ cm, then it remains constant. This result agrees well with results obtained with the probe for longer distances. For the purposes of the present article, the plasma characteristics that are far from the target are of importance, since splashing is significantly reduced at such distances, films with a very smooth morphology can be obtained.

The Langmuir Probe was used to obtain the TOF spectra of ions and their density, at different distances from the target. Fig. 2 shows a typical set of curves obtained for a fixed value of laser fluence and different distances from 8 to 15 cm from the target. From these spectra the mean kinetic energy of ions was obtained, following the procedure described in Ref. [9]. The plasma density values were obtained from the peak values of current of the TOF curves. Fig. 3 shows the mean ion kinetic energy as a function of the distance from the target, for different values of laser fluence. The ion energy remains practically constant for each value of fluence. For the highest fluence ($6\ \mathrm{J/cm^2}$) the highest ion energy (between 450 and 500 eV) was obtained. The lowest values of ion energy, of approximately 120 eV, were obtained for the low laser fluence. It is worth noting that a small increase in energy with distance was observed. Other groups have observed this behaviour; particularly when higher (than in our case) fluences are employed [see e.g. [9,10]], and can be explained in terms of the existence of an acceleration mechanism inside the plasma due to the violation of the plasma quasi-neutrality, leading to the formation of an electric field, which accelerates ions. This can be observed in the TOF curves as a fast peak in front of the main ion peak (see Fig. 2). Fig. 4 shows the plasma density as a function of the distance from the target, for different values of laser fluence. It is seen from this plot that a higher flux and a smaller distance from the target, results in a higher plasma density. In the range of distances studied with the probe the plasma density also depends on the working pressure; it decreases as the pressure is increased. Similarly, the plasma plume reduces in its dimensions and is confined to a smaller space. Furthermore, the total number of ionized particles that can escape from the region of the plasma plume is reduced as the pressure is increased. On the other hand, probe measurements carried out outside the plasma plume (from 6 to 15 cm from the target), at different working pressures (from 1×10^{-3} to 1.3 Pa), where the mean free path of ions with relatively high energy ($>$ 80 eV) [11], is many times larger than the length of our working chamber ($\sim$20 cm), showed that the ion energy has only a small dependence on the pressure, the variation for a fixed laser fluence was not greater than 50 eV.

The above results show that for the conditions in which the ablation of the carbon target is carried out in this work, there is a wide range of ion energies and plasma densities in which we can expect the formation of amorphous carbon thin films with different content of sp^3 C hibridisation.

3.2. Thin film deposition

Fig. 5 shows Ion energy – Plasma density diagram obtained by combining Figs. 3 and 4. This diagram was

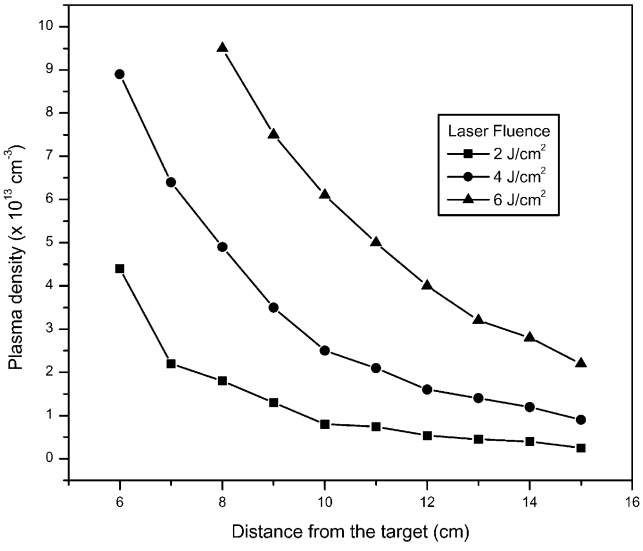

Fig. 4. Plasma density as a function of the distance from the target for different values of laser fluence.

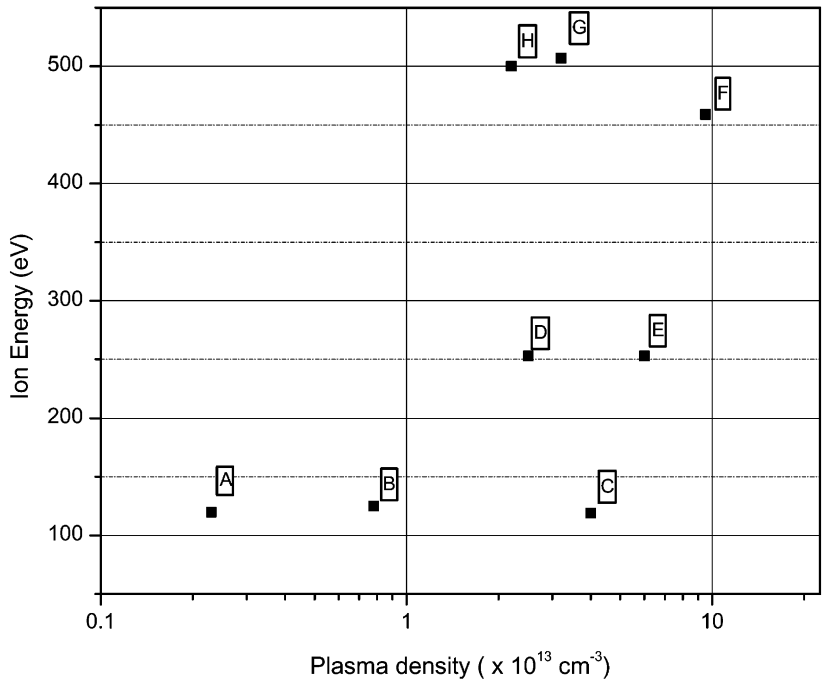

Fig. 5. Mean ion energy – Plasma density diagram, showing the experimental conditions under which samples were prepared.

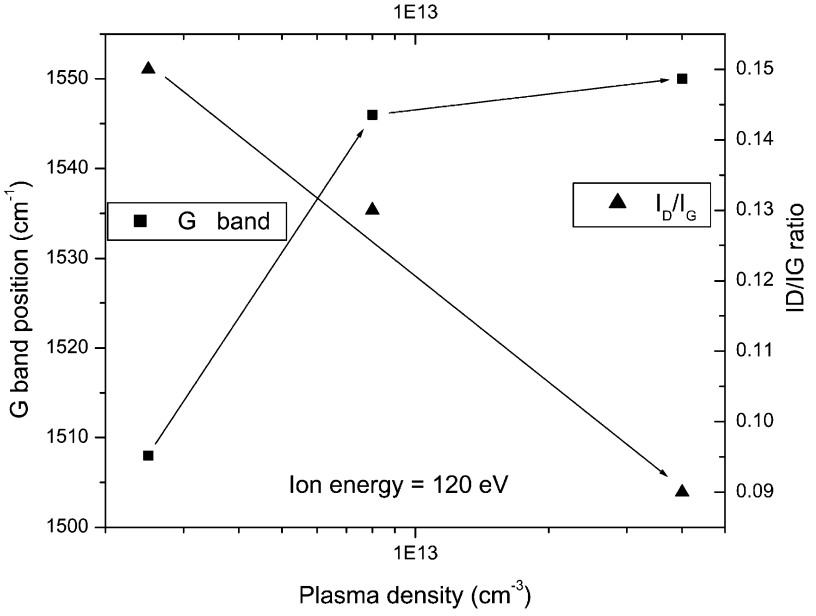

Fig. 6. Position of the Raman G peak and value of the ratio I_D/I_G as a function of the plasma density. The ion energy is kept constant at a value of 120 eV.

used to determine the plasma conditions under which deposition of films were to be carried out. For example, point F, in Fig. 5, means that sample number F, was deposited with a mean ion kinetic energy close to 450 eV and a plasma density equal to 9.5×10^{13} cm^{-3}, and so on. From this figure, it can be seen that three levels of ion energy were used. A high level with ion energy around 450 eV, a medium level with energies around 250 eV and a low one in which the ion energy had a value close to 120 eV. For each level of ion energy different values of plasma density were used to prepare the samples.

We used Raman spectroscopy to study the variation in the characteristic peaks D and G of amorphous carbon as a function of the deposition conditions. The Raman spectra were interpreted in terms of the model proposed

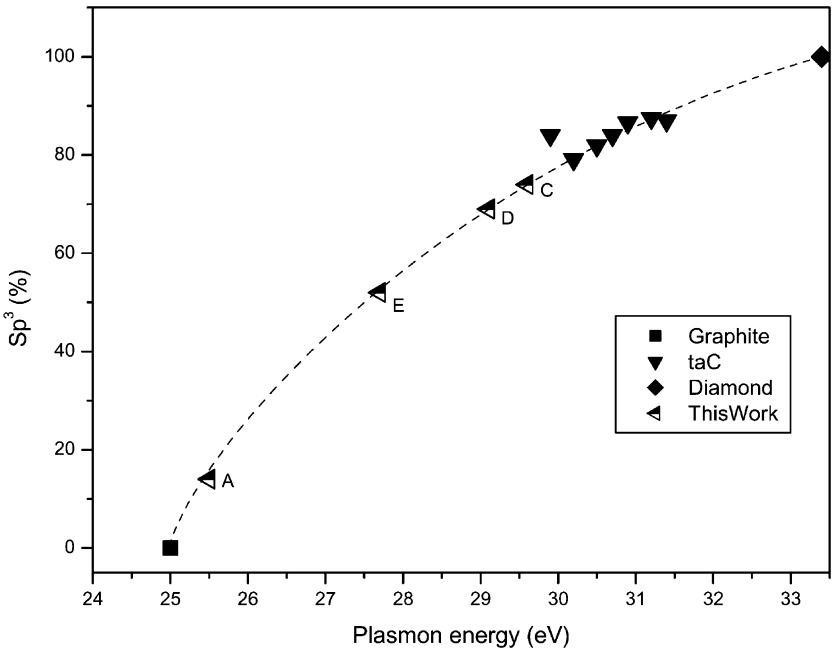

Fig. 7. Sp^3 content as a function of the plasmon energy. For ta-C data were taken from [13]. The dashed line is a guide for the eye.

by Ferrari and Robertson [12]. For this model, a Breit-Wigner-Fano + Lorentzian fitting was used to obtain the relation I_D/I_G (as the ratio of the peak heights) and the G peak position. Fig. 6 shows the variation of these quantities for the case of samples deposited at low fluence (i.e. low ion energy, samples A, B and C in Fig. 5) with different values of plasma density. From this plot, it can be seen that when the plasma density is increased (the ion energy is constant at 120 eV), the ratio I_D/I_G tends to decrease and the position of the G peak tends to increase. In other words, in this case as the plasma density increases the sp^3 content in the film also tends to increase. For the case of the highest energies (samples F, G and H in Fig. 5), the I_D/I_G ratio and the position of the G peak both tend to increase with the initial increase in the plasma density, but furthermore increases in the density causes the I_D/I_G ratio to decrease, and the position of the G peak to have only a small increase. This situation can be interpreted as follows: for the lowest plasma densities (with the energy at a high level) a polycrystalline graphite-like material without sp^3 is formed, and with further increases in the plasma density the deposit becomes amorphous with preferential sp^2 bonding with a very low sp^3. Therefore, it might be expected that at high ion energies, it was not possible to obtain a film with high sp^3 content. When the plasma density is fixed at 5×10^{13} cm^{-3} and the ion energy is increased from the low level values to the medium level values (samples C and D), I_D/I_G tends to decrease and the peak G moves to higher values. A further increase in ion energy reverses this tendency (samples D and G); I_D/I_G begins to increase and the G peak moves to smaller values. Therefore, in this case the sp^3 content in the film slightly increases as the ion energy is increased up to the medium level value close to 250 eV, and at higher ion energies, the excess energy promotes thermal relaxation reducing the effectiveness of the sp^2 to sp^3 transformation.

In order to verify the above-discussed Raman results, a few samples made under a selection of the conditions indicated in Fig. 5, were analysed using Electron Energy Loss Spectroscopy. These results were compared to results from other authors [13], as shown in Fig. 7. This figure shows the sp^3 content as a function of the plasmon energy. According to the Raman analysis, sample A should have sp^3 content less than sample C, and sample D should have the same or slightly less sp^3 content than sample C, this is in good agreement with EELS measurements shown in Fig. 7.

4. Conclusions

Analysis of the plasma plume produced by laser ablation of a carbon target revealed the presence of carbon ions with energies ranging from 100 to 500 eV, with different plasma densities depending on the target-substrate distance. Under these conditions amorphous carbon thin films with different sp^3 contents were deposited. The overall behaviour showed that the highest sp^3 content is obtained when the lowest ion energy is used ($\sim$120 eV) together with the highest obtainable plasma density, i.e. when the lowest laser fluence is

used. When the ion energy is increased, the plasma density must be reduced to improve the sp^3 content. A further increase in the ion energy produces films with low sp^3 bonding even when the lowest plasma densities are used.

Acknowledgments

The present work was supported by the Consejo Nacional de Ciencia y Tecnología of Mexico under contracts 29250-E and 33873-E.

References

[1] D.R. Mckenzie, Rep. Prog. Phys. 59 (1996) 1611.
[2] R. Silva, G.A.J. Amaratunga, J. Robertson, W.I. Milne (Eds.), Amorphous Carbon – State of the Art, World Scientific, Singapore, 1998.
[3] T. Yoshitake, H. Aoki, K. Suizu, K. Takahashi, K. Nagayama, Appl. Surf. Sci. 141 (1999) 129.
[4] Voevodin, M.S. Donley, J.S. Zabinski, Surf. Coat. Technol. 92 (1997) 42.
[5] J. Robertson, MRS Symp. Proc. 508 (1998).
[6] Y. Lifshitz, S.R. Kasi, J.W. Rabalais, Phys. Rev. Lett. 62 (1989) 1290.
[7] J. Robertson, Diamond Rel. Mater. 3 (1994) 361.
[8] L. Escobar-Alarcón, M. Villagrán, E. Haro-Poniatowski, J.C. Alonso, M. Fernández-Guasti, E. Camps, Appl. Phys. A 69 (1999) s583.
[9] N.M. Bulgakova, A.V. Bulgakov, Oleg, F. Bobrenok, Phys. Rev. E 62 (2000) 5624.
[10] J.S. Pearlman, J.J. Thomson, C.E. Max, Phys. Rev. Lett. 54 (1977) 1397.
[11] Y.P. Raizer, Gas Discharge Physics, Springer-Verlag, 1997.
[12] C. Ferrari, J. Robertson, Phys. Rev. B 61 (2000) 14095.
[13] A.C. Ferrari, A. Libassi, B.K. Tanner, V. Stolojan, J. Yuan, S.E. Rodil, B. Kleinsorge, J. Robertson, Phys. Rev. B62 (2000) 11089.